

**INTERNATIONAL JOURNAL OF SCIENCE FOR GLOBAL SUSTAINABILITY****Effect of Water Insoluble Component on Angstrom Exponent and Radiative Forcing of Continental Polluted Aerosols***Bello, M.¹, Yusuf, Y.², Sa'adu, L.¹, Abdulmuminu, I.¹, and Maduka, N. C.¹¹Department of Physics, Federal University Gusau, Zamfara State, Nigeria²Department of Physics, Zamfara College of Arts and Science, Gusau, Zamfara State, NigeriaCorresponding Authors Email Address: ridmann2016@gmail.com Phone no.: +2348062214994

Received on: January, 2020

Revised and Accepted on: March 2020

Published on: March 2020

ABSTRACT

In this paper, the optical properties of continental polluted aerosols were extracted from optical properties of Aerosols and cloud (OPAC) software at a spectral range of (0.24-0.80) μm ultraviolet to visible region and at eight relative humidity (0%, 50%, 70%, 80%, 90%, 95%, 98% & 99%) to determine the effect of water insoluble component. The data were obtained by varying default concentration number of water insoluble component in the simulation software (OPAC). The optical parameters extracted were used to calculate the radiative forcing by the approach of Chylek and Wong, the Angstrom exponent (α), turbidity (β) and curvature (α_2) using regression analysis. From the results obtained it was observed that α which determined the particle size distribution is greater than 1.0 at (0%-95%) RHs and it signifies that fine accumulation mode is the most dominant but at deliquescence points (98%-99%) RHs α is less than 1.0 and this show the present of coarse mode. The curvature α_2 which gives additional information of particle mode distributions was negative at all RHs indicating the dominance of fine mode particles. The optical depth of the atmospheric aerosols were determined for each model and analyzed graphically, the results have shown the clear decrease in size with increase in wavelength, but increases with increase in RHs. The turbidity β increase with increases in concentration number of water insoluble signifies the increases in aerosol loading which show decrease in visibility of the atmosphere. The analysis further shows that these aerosols have monomodal type of particle distributions.

Keyword: Angstrom exponent, Curvature, Optical depth, Radiative forcing, Turbidity.**1.0 INTRODUCTION**

Aerosol science returned to prominence in the last decade due to clear evidence of anthropogenic impacts and the important role of aerosols in the radiative forcing of climate. (Pan *et al.*, 2009).

The climatic and environmental effects of atmospheric aerosols are the critical issues in global science community because aerosols, derived from natural and anthropogenic emission sources, are well known to affect the air quality, human health, and radiation budget (IPCC, 2007).

Uncertainty in quantifying the climatic impacts of aerosols continues to be greater than that of greenhouse gases due to variety of their sources, varying trends in aerosol loading and extreme

heterogeneity in the spatial and temporal variability of their optical and microphysical properties (Smirnov *et al.* 2002). The interplay between water vapor and aerosol particles has gained great attention over recent decades due to the key roles it plays in air quality and climate change. To date, some scientific issues, such as particle hygroscopicity and its effect on the optical properties of aerosol and CCN activation, are relatively well recognized (Zhijun *et al.*, 2018).

Therefore, the accurate assessment of the aerosol impact on radiative transfer is a complex task, since various aerosol types cause different effects on the solar radiation spectral distribution. Thus, detailed knowledge of the optical properties of the key aerosol types is highly essential (Kumar *et al.* 2014).

Aerosols directly affect the Earth's radiation balance by scattering and absorbing radiation within the atmosphere. Enhanced backscattering of solar radiation due to increasing aerosol concentrations has an atmospheric cooling effect that can rival atmospheric warming due to greenhouse gases. Aerosols, acting as cloud condensation nuclei, indirectly alter the microphysical and optical properties of clouds, enhancing cloud albedo, increasing cloud lifetime and thereby suppressing precipitation (Mulcahy *et al.*, 2009).

The water insoluble part of aerosol particles consists mostly of soil particles with a certain amount of organic material (Hess *et al.*, 1998). Numerous studies have investigated the relationship between aerosol scattering and relative humidity RH in terms of Radiative forcing and Angstrom coefficients.

The effective hygroscopic growths and effective radii were parameterized and the modified Köhler equation was used to determine water activities, Kelvin effects and humidification factors. It was

2.0 MATERIALS AND METHOD

The data used for continental polluted aerosols shown in Table 1: were extracted from the optical properties of aerosols and clouds (OPAC) 4.0 dataset. Mixtures of three components were used to describe continental average. They are: water

observed that the data fitted the models very well. The results show that the growth factor and effective radii increases with increase in RH and are more pronounced at 90-99% RHs, the water activities is more dominant than the Kelvin effect in all types of models (Muhammad, 2017). The Angstrom exponent and turbidity of water soluble components in the radiative forcing of urban aerosols was performed and the analysis of RF, AOD and g verify that the water soluble components of urban aerosols reflect cooling effect, the α and α show that earth's atmosphere is composed of both fine and coarse mode particles in which fine mode particles in dominant in the urban region (Bala, 2017). The aim of this paper is to model the effect of varying concentration number of water insoluble components on the radiative forcing of Continental polluted aerosols on three components of aerosols extracted from OPAC 4.0 software package at eight relative humidities of (0%, 50%, 70%, 80%, 90%, 95%, 98% and 99%), and at spectral range of (0.25 - 0.80 μm) to determine radiative forcing as well as Angstrom coefficients.

soluble components, consist of scattering aerosols, which are hygroscopic in nature, such as sulfates and nitrates present in anthropogenic pollution, while water insoluble and soot are considered not soluble in water and therefore the particles are assumed not to grow with increasing relative humidity.

Table 1; given describes the concentrations of continental polluted aerosols simulated with varying water insoluble concentrations $N_i(1/\text{cm}^3)$ (Hess *et al.*, 1998).

Components	Model 1	Model 2	Model 3	Model 4	Model 5
Water soluble (WASO)	15700	15700	15700	15700	15700
Water insoluble (INSO)	0.6	0.8	1.0	1.2	1.4
Soot	34300	34300	34300	34300	34300

2.1 Radiative Forcing Model

To estimate the radiative forcing using simple model, we adopt the approach used by

$$\Delta F_R = -\frac{S_0}{4} T_{atm}^2 (1 - N) \{ (1 - A)^2 2\beta \tau_{sca} - 4A\tau_{abs} \} \quad 1$$

where S_0 is the solar constant, T_{atm} is the transmittance of the atmosphere above the aerosol layer, N_{cloud} is the fraction of the sky covered by clouds, τ is the aerosol optical depth, A is the average single scattering albedo of the

Chylek and Wong (1995) from which the global averaged direct aerosol radiative forcing ΔF_R is given by:

aerosol layer, and β is the fraction of radiation scattered by aerosol into the atmosphere while τ_{sca} and τ_{abs} are the aerosol layer scattering and absorption optical thickness respectively. The above expression gives the radiative forcing due

to the change of reflectance of the earth-aerosol system.

The up-scattering fraction is calculated using an approximate relation (Sagan and Pollack,1967)

$$\beta = \frac{1}{2}(1 - g) \quad 2$$

2.2 Estimation of Angstrom Coefficients

The spectral behavior of the aerosols optical depth (τ) that expresses the spectral dependence of any of the optical parameters with the wavelength of light (λ) as inverse power law (Angstrom, 1961; Angstrom, 1929):

$$(\lambda) = \beta \lambda^{-\alpha} \quad 3$$

The wavelength dependence of (λ) can be characterized by the Ångström parameter, which is a coefficient of the following regression:

$$\ln\tau(\lambda) = -\alpha \ln(\lambda) + \ln\beta \quad 4$$

Where β and α are the turbidity coefficient and Ångström exponent (Liou, 2002; O’Neill and Roer,1993) α is related to the size distribution.

The Angstrom exponent itself varies with wavelength, and a more precise empirical relationship between aerosol extinction and wavelength is obtained with a 2nd-order polynomial (King and Byrne, 1976) as:

$$\ln\tau(\lambda) = \alpha_2(\ln\lambda)^2 + \alpha_1 \ln\lambda + \ln\beta \quad 5$$

The coefficient α_2 accounts for “curvature” often observed in Sun photometry measurements. In case of negative curvature ($\alpha_2 < 0$, convex type

Where g is the asymmetry parameter of the aerosol layer. The model parameters are assigned the following values: $S_0=1368 \text{ Wm}^{-2}$, $T_{\text{atm}}= 0.79$, (Penner *et al.*, 1992) and cloudness $N=0.6$. The global averaged albedo $A=0.22$ over land and $A=0.06$ over the ocean with 80% of aerosols being over the land.

curves) the rate of change of α is more significant at the longer wavelengths, while positive curvature ($\alpha_2 > 0$, concave type curves) the rate of change of α is more significant at the shorter wavelengths. Eck *et al.*, (1999) reported the existence of negative curvatures for fine mode and positive curvatures for significant contribution by coarse mode particles in the size distribution.

3.0 RESULTS AND DISCUSSION

The results of Angstrom exponent and radiative forcing for water insoluble component of atmospheric aerosols models extracted from optical properties of aerosols and cloud (OPAC) 4.0. The effect of water insoluble component on optical depth, scattering coefficient, absorption coefficient and asymmetry parameter at spectral range of 0.25 to 0.80 μm near Ultraviolet to Visible region for eight relative humidities (RHs) (0%,50%,70%,80%,90%,95%,98%&99%) of continental polluted aerosols were obtained and shown on the tables and figures below.

Table 2a: Linear results of the regression analysis for model 1 of table 1

RH(%)	R ²	Sig	A	Sig	β	Sig
0	0.9910	1.44E-11	1.2213	1.44E-11	0.1607	2.49E-14
50	0.9900	2.45E-11	1.2191	2.45E-11	0.2313	3.82E-13
70	0.9892	3.61E-11	1.2033	3.61E-11	0.2781	1.90E-12
80	0.9885	4.97E-11	1.1825	4.97E-11	0.3305	9.26E-12
90	0.9867	1.03E-10	1.1293	1.03E-10	0.4664	4.86E-10
95	0.9840	2.60E-10	1.0526	2.60E-10	0.6979	8.36E-07
98	0.9791	9.78E-10	0.9321	9.78E-10	1.2138	1.98E-04
99	0.9745	2.66E-09	0.8450	2.66E-09	1.7566	1.39E-08

Based on the content of Table 2a and by observing the values R² and the significance of all coefficients, it can be said that the data fitted the equation model very well. The value α increases with the RHs and this signifies the increase in the dominance of

fine/accumulation particles, but at deliquescence point (98-99%) RH it is less than 1 signifies the presence of coarse mode particles as fine mode are act as cloud condensation nuclei. But β (turbidity coefficient)

increase with the increase in RHs indicating that the aerosol loading also increases with the increase in RH.

Table 2b: Quadratic result of the regression analysis for model 1 of table 1

RH(%)	R ²	Sig	α_1	Sig	α_2	Sig	β	Sig
0	0.9998	2.47E-17	-1.7674	3.56E-13	-0.3493	1.05E-08	0.1360	7.35E-18
50	0.9999	6.01E-19	-1.7982	7.36E-15	-0.3703	1.57E-10	0.1938	1.03E-18
70	0.9999	1.51E-19	-1.7986	1.65E-15	-0.3807	2.79E-11	0.2319	6.54E-19
80	1.0000	2.97E-20	-1.7874	2.95E-16	-0.3869	4.10E-12	0.2748	3.34E-19
90	1.0000	2.45E-21	-1.7520	1.94E-17	-0.3982	1.76E-13	0.3857	2.85E-19
95	1.0000	1.48E-22	-1.6903	8.69E-19	-0.4078	4.61E-15	0.5745	1.21E-18
98	1.0000	2.14E-23	-1.5785	8.00E-20	-0.4133	2.03E-16	0.9965	5.41E-02
99	1.0000	5.89E-23	-1.4940	1.52E-19	-0.4151	2.27E-16	1.4410	2.96E-18

From Table 2b and by observing the values R² and the significance of all coefficients, it can be said that the data fitted the equation model very well. The increase of α_2 with RHs signifies the increase in the dominance of fine/accumulation

modes particles. The negative sign of α_2 , shows that this is monomodal and is dominated by fine mode particles. But β (turbidity coefficient) increases with the increase in RHs, indicating a relatively hazy and atmosphere.

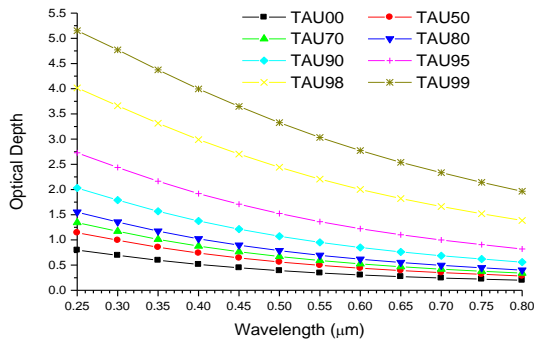


Figure 2(a). A graph of optical depth against wavelength for model 1 of table 1

From the plots of figure 2a, it can be seen that the optical depth follow a relatively smooth decrease with the increase in wavelength though some are steeper than others and the steepness increases with the increase in relative humidities.

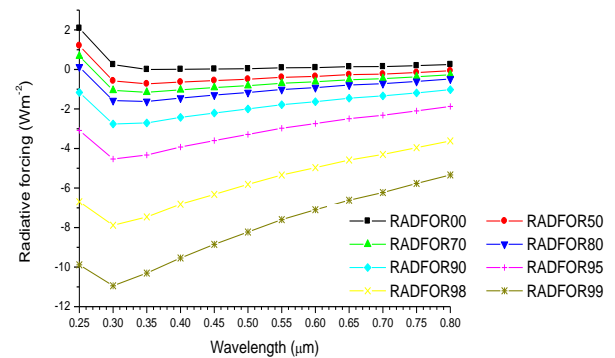


Figure 2(b). A graph of RF against wavelength for model 1 of table 3.6

From the plots of figure 2b, it can be seen that the radiative forcing decreases with increase in relative humidities. Also, at 0% to 80% RHs the radiative forcing indicate warming effect while from 90% to 99% indicate cooling effect and both effects increase from 0.25 to 0.30 μ m and increase with increase in wavelength and decrease in relative humidities and this show that adding water insoluble reflects warming on the earth atmosphere.

Table 3a: Linear results of the regression analysis for model 2 of table 1

RH(%)	R ²	Sig	α	Sig	β	Sig
0	0.9917	9.90E-12	1.1988	9.90E-12	0.1664	1.72E-14
50	0.9905	1.92E-11	1.2031	1.92E-11	0.2371	3.12E-13
70	0.9897	2.88E-11	1.1901	2.88E-11	0.2839	1.59E-12
80	0.9888	4.35E-11	1.1715	4.35E-11	0.3362	8.63E-12
90	0.9869	9.54E-11	1.1218	9.54E-11	0.4723	4.94E-10
95	0.9842	2.47E-10	1.0477	2.47E-10	0.7038	9.50E-07
98	0.9793	9.51E-10	0.9291	9.51E-10	1.2201	1.53E-04
99	0.9747	2.60E-09	0.8432	2.60E-09	1.7627	1.25E-08

From Table 3a and by observing the values R² and the significance of all coefficients, it can be said that the data fitted the equation model very well. The value α increases with the RHs and this signifies the increase in the dominance of

fine/accumulation particles, but at deliquescence point (98-99%) RH it is less than 1 signifies the presence of coarse mode particles as fine mode are act as cloud condensation nuclei. But β (turbidity coefficient) increase with the increase in RHs indicating that the aerosol loading also increases with the increase in RH.

Table 3b: Quadratic result of the regression analysis for model 2 of table 1

RH(%)	R ²	Sig	α_1	Sig	α_2	Sig	β	Sig
0	0.9998	4.67E-17	-1.7135	7.49E-13	-0.3292	2.78E-08	0.1422	1.43E-17
50	0.9999	1.14E-18	-1.7604	1.50E-14	-0.3564	3.72E-10	0.2000	2.06E-18
70	0.9999	1.82E-19	-1.7655	2.12E-15	-0.3680	4.10E-11	0.2382	8.37E-19
80	0.9999	5.17E-20	-1.7626	5.34E-16	-0.3780	8.06E-12	0.2807	6.21E-19
90	1.0000	5.55E-21	-1.7352	4.51E-17	-0.3923	4.26E-13	0.3916	7.00E-19
95	1.0000	2.36E-22	-1.6789	1.41E-18	-0.4037	7.72E-15	0.5805	2.19E-18
98	1.0000	1.86E-23	-1.5714	7.03E-20	-0.4108	1.81E-16	1.0030	8.81E-02
99	1.0000	2.48E-23	-1.4892	6.47E-20	-0.4132	9.77E-17	1.4473	1.10E-18

From Table 3b and by observing the values R² and the significance of all coefficients, it can be said that the data fitted the equation model very well. The negative sign of α_2 , shows that this is monomodal and is dominated by fine mode particles. The increase in the values of α_2 , with

RH shows the increase in the concentrations of fine particles. But β (turbidity coefficient) increase with the increase in RH indicating that the aerosol loading also increases with the increase in RH.

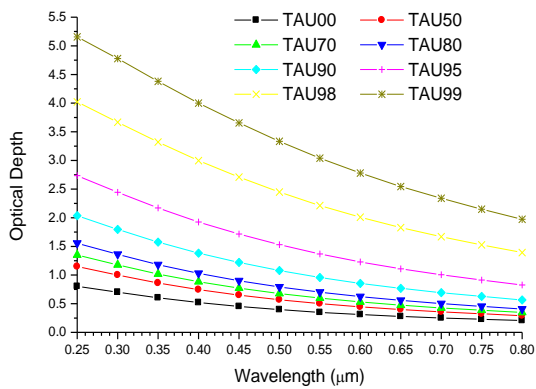


Figure 3(a). A graph of optical depth against wavelength for model 2 of table 1

From the plots of figure 3a, it can be seen that the optical depth follow a relatively smooth decrease with the increase in wavelength though some are steeper than others and the steepness increases with the increase in relative humidities.

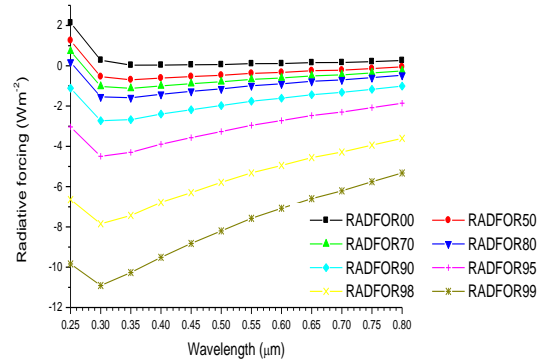


Figure 3(b). A graph of RF against wavelength for model 2 of table 1

From the plots of figure 3b, it can be seen that the radiative forcing decreases with increase in relative humidities. Also, at 0% to 80% RHs the radiative forcing indicate warming effect while from 90% to 99% indicate cooling effect and both effects increase from 0.25 to 0.30μm and increase with increase in wavelength and decrease in relative humidities and this show that adding water insoluble reflects warming on the earth atmosphere.

Table 4a: Linear results of the regression analysis for model 3 of table 1

RH(%)	R ²	Sig	A	Sig	β	Sig
0	0.9922	6.91E-12	1.1773	6.91E-12	0.1721	1.21E-14
50	0.9910	1.47E-11	1.1882	1.47E-11	0.2428	2.48E-13
70	0.9900	2.41E-11	1.1773	2.41E-11	0.2897	1.40E-12
80	0.9892	3.66E-11	1.1606	3.66E-11	0.3421	7.74E-12
90	0.9872	8.52E-11	1.1137	8.52E-11	0.4782	4.86E-10
95	0.9843	2.34E-10	1.0425	2.34E-10	0.7099	1.09E-06
98	0.9794	9.30E-10	0.9262	9.30E-10	1.2263	1.20E-04
99	0.9747	2.57E-09	0.8411	2.57E-09	1.7691	1.14E-08

Considering Table 4a and by observing the values R² and the significance of all coefficients, it can be said that the data fitted the equation model very well. The value α increases with the RHs and this signifies the increase in the dominance of fine/accumulation particles, but at deliquescence

point (98-99%) RH it is less than 1 signifies the presence of coarse mode particles as fine mode are act as cloud condensation nuclei. But β (turbidity coefficient) increase with the increases in RHs indicating that the aerosol loading also increases with the increase in RH.

Table 4b: Quadratic result of the regression analysis for model 3 of table 1

RH(%)	R ²	Sig	α_1	Sig	α_2	Sig	β	Sig
0	0.9997	8.08E-17	-1.6633	1.43E-12	-0.3108	6.66E-08	0.1484	2.57E-17
50	0.9999	1.92E-18	-1.7234	2.73E-14	-0.3422	7.98E-10	0.2062	3.67E-18
70	0.9999	3.57E-19	-1.7360	4.39E-15	-0.3573	9.46E-11	0.2443	1.75E-18
80	0.9999	9.82E-20	-1.7357	1.07E-15	-0.3678	1.79E-11	0.2870	1.27E-18
90	1.0000	6.83E-21	-1.7158	5.75E-17	-0.3850	5.81E-13	0.3979	9.43E-19
95	1.0000	1.91E-22	-1.6673	1.16E-18	-0.3995	6.56E-15	0.5867	2.02E-18
98	1.0000	2.40E-23	-1.5651	9.12E-20	-0.4086	2.38E-16	1.0091	2.80E-04
99	1.0000	2.51E-23	-1.4849	6.57E-20	-0.4117	9.98E-17	1.4536	9.79E-19

From Table 4b and by observing the values R² and the significance of all coefficients, it can be said that the data fitted the equation model very well. The negative sign of α_2 , shows that this is monomodal and is dominated by fine mode particles. The increase in the values of α_2 , with

RH shows the increase in the concentrations of fine particles. But β (turbidity coefficient) increase with the increase in RH indicating that the aerosol loading also increases with the increase in RH.

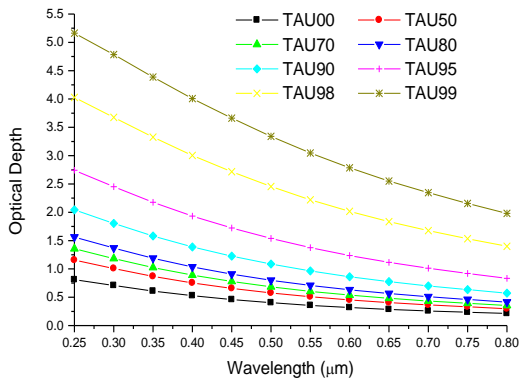


Figure 4(a). A graph of optical depth against wavelength for model 3 of table 1

From the plots of figure 4a, it can be seen that the optical depth follow a relatively smooth decrease with the increase in wavelength though some are steeper than others and the steepness increases with the increase in relative humidities.

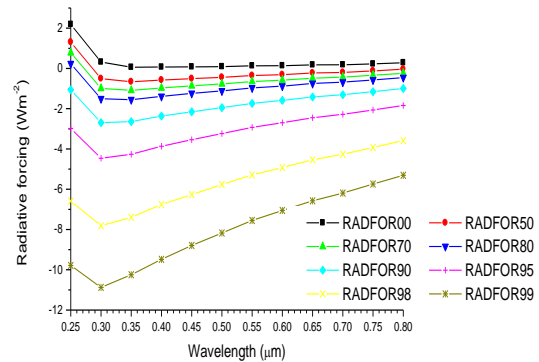


Figure 4(b). A graph of radiative forcing against wavelength for model 3 of table 1

From the plots of figure 4b, it can be seen that the radiative forcing decreases with increase in relative humidities. Also, at 0% to 80% RHs the radiative forcing indicate warming effect while from 90% to 99% indicate cooling effect and both effects increase from 0.25 to 0.30 μ m and increase with increase in wavelength and decrease in relative humidities and this show that adding water insoluble reflects warming on the earth atmosphere.

Table 5a: Linear results of the regression analysis for model 4 of table 1

RH(%)	R ²	Sig	A	Sig	β	Sig
0	0.9928	4.90E-12	1.1566	4.90E-12	0.1779	8.68E-15
50	0.9914	1.17E-11	1.1731	1.17E-11	0.2486	2.04E-13
70	0.9904	1.99E-11	1.1647	1.99E-11	0.2955	1.22E-12
80	0.9895	3.12E-11	1.1503	3.12E-11	0.3478	7.06E-12
90	0.9875	7.60E-11	1.1063	7.60E-11	0.4841	4.78E-10
95	0.9846	2.17E-10	1.0374	2.17E-10	0.7159	1.21E-06
98	0.9796	8.83E-10	0.9233	8.83E-10	1.2325	9.22E-05
99	0.9748	2.51E-09	0.8391	2.51E-09	1.7755	1.02E-08

From Table 5a and by observing the values R² and the significance of all coefficients, it can be said that the data fitted the equation model very well. The value α increases with the RHs and this signifies the increase in the dominance of fine/accumulation particles, but at deliquescence

point (98-99%) RH it is less than 1 indicating the presence of coarse mode particles as fine mode are act as cloud condensation nuclei. But β (turbidity coefficient) increase with the increase in RHs indicating that the aerosol loading also increases with the increase in RH.

Table 5b: Quadratic result of the regression analysis for model 4 of table 1

RH(%)	R ²	Sig	α_1	Sig	α_2	Sig	β	Sig
0	0.9997	1.34E-16	-1.6163	2.61E-12	-0.2939	1.51E-07	0.1546	4.40E-17
50	0.9999	3.32E-18	-1.6885	5.04E-14	-0.3296	1.70E-09	0.2124	6.68E-18
70	0.9999	6.73E-19	-1.7063	8.75E-15	-0.3464	2.13E-10	0.2505	3.51E-18
80	0.9999	1.50E-19	-1.7111	1.71E-15	-0.3586	3.15E-11	0.2931	2.08E-18
90	1.0000	8.21E-21	-1.6974	7.16E-17	-0.3780	7.75E-13	0.4042	1.24E-18
95	1.0000	3.45E-22	-1.6542	2.16E-18	-0.3945	1.27E-14	0.5931	4.20E-18
98	1.0000	2.82E-23	-1.5569	1.09E-19	-0.4052	2.93E-16	1.0158	4.23E-06
99	1.0000	2.35E-23	-1.4797	6.21E-20	-0.4096	9.55E-17	1.4603	8.03E-19

From Table 5b and by observing the values R² and the significance of all coefficients, it can be said that the data fitted the equation model very well. The negative sign of α_2 , show that this is monomodal and is dominated by fine mode particles. The increase in the values of α_2 , with

RH shows the increase in the concentrations of fine particles. But β (turbidity coefficient) increase with the increase in RH indicating that the aerosol loading also increases with the increase in RH.

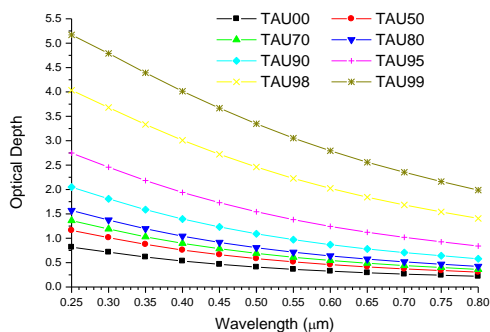


Figure 5(a). A graph of optical depth against wavelength for model 4 of table 1

From the plots of figure 5a, it can be seen that the optical depth follow a relatively smooth decrease with the increase in wavelength though some are steeper than others and the steepness increases with the increase in relative humidities.

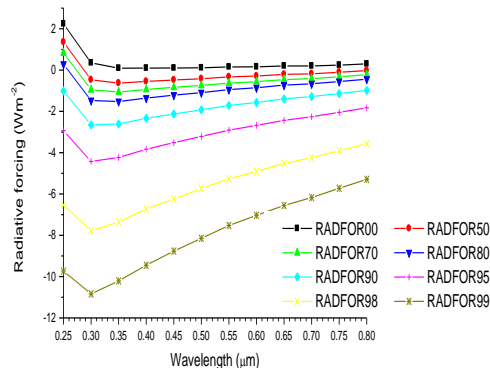


Figure 5(b). A graph of radiative forcing against wavelength for model 4 of table 1

From the plots of figure 5b, it can be seen that the radiative forcing decreases with increase in relative humidities. Also, at 0% to 80% RHs the radiative forcing indicate warming effect while from 90% to 99% indicate cooling effect and both effects increase from 0.25 to 0.30μm and increase with increase in wavelength and decrease in relative humidities and this show that adding water insoluble reflects warming on the earth atmosphere.

Table 6a: Linear results of the regression analysis for model 5 of table 1

RH(%)	R ²	Sig	A	Sig	β	Sig
0	0.9933	3.38E-12	1.1365	3.38E-12	0.1837	6.06E-15
50	0.9918	9.34E-12	1.1583	9.34E-12	0.2544	1.71E-13
70	0.9908	1.61E-11	1.1527	1.61E-11	0.3013	1.04E-12
80	0.9899	2.63E-11	1.1397	2.63E-11	0.3537	6.36E-12
90	0.9877	6.82E-11	1.0988	6.82E-11	0.4899	4.74E-10
95	0.9847	2.06E-10	1.0324	2.06E-10	0.7219	1.40E-06
98	0.9797	8.63E-10	0.9204	8.63E-10	1.2388	7.24E-05
99	0.9749	2.46E-09	0.8372	2.46E-09	1.7818	9.22E-09

From Table 6a and by observing the values R² and the significance of all coefficients, it can be said that the data fitted the equation model very well. The value α increases with the RHs and this signifies the increase in the dominance of fine/accumulation particles, but at deliquescence

point (98-99%) RH it is less than 1 signifies presence of coarse mode particles as fine mode are act as cloud condensation nuclei. But β(turbidity coefficient) increase with the increase in RHs indicating that the aerosol loading also increases with the increase in RH.

Table 6b: Quadratic result of the regression analysis for model 5 of table 1

RH(%)	R ²	Sig	α_1	Sig	α_2	Sig	β	Sig
0	0.9997	2.04E-16	-1.5698	4.39E-12	-0.2771	3.22E-07	0.1610	6.94E-17
50	0.9999	5.19E-18	-1.6555	8.35E-14	-0.3179	3.24E-09	0.2186	1.10E-17
70	0.9999	9.83E-19	-1.6772	1.36E-14	-0.3354	3.76E-10	0.2567	5.48E-18
80	0.9999	2.56E-19	-1.6855	3.07E-15	-0.3490	6.28E-11	0.2994	3.81E-18
90	1.0000	1.61E-20	-1.6795	1.45E-16	-0.3713	1.67E-12	0.4104	2.67E-18
95	1.0000	6.04E-22	-1.6433	3.83E-18	-0.3906	2.32E-14	0.5991	8.39E-18
98	1.0000	3.69E-23	-1.5504	1.44E-19	-0.4029	3.92E-16	1.0221	3.24E-07
99	1.0000	2.31E-23	-1.4750	6.14E-20	-0.4079	9.56E-17	1.4667	6.96E-19

Based on the contents of Table 6b and by observing the values R² and the significance of all coefficients, it can be said that the data fitted the equation model very well. The negative sign of α_2 , shows that this is monomodal and is dominated by fine mode particles. The increase in

the values of α_2 , with RH shows the increase in the concentrations of fine particles. But β (turbidity coefficient) increase with the increase in RH indicating that the aerosol loading also increases with the increase in RH.

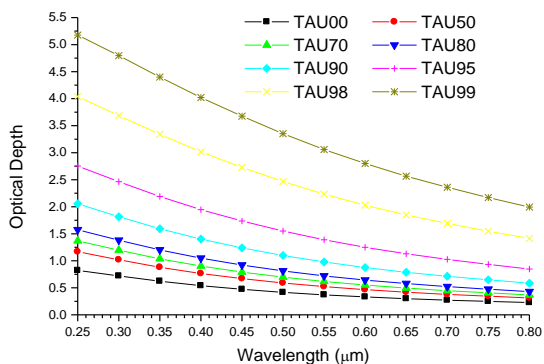


Figure 6(a). A graph of optical depth against wavelength model 5 of table 1

From the plots of figure 6a, it can be seen that the optical depth follow a relatively smooth decrease with the increase in wavelength though some are steeper than others and the steepness increases with the increase in relative humidities.

From the plots of figure 4.30b, it can be seen that the radiative forcing decreases with increase in

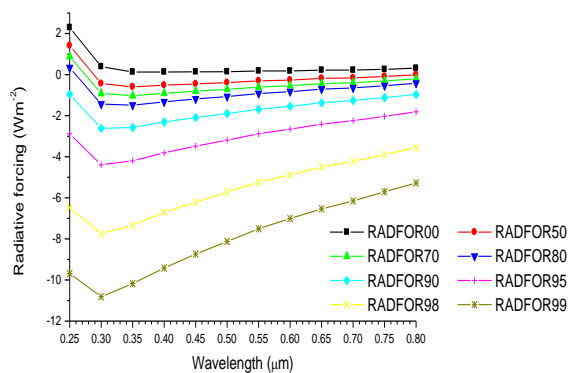


Figure 6(b). A graph of radiative forcing against wavelength for model 5 of table 1

relative humidities. Also, at 0% to 80% RHs the radiative forcing indicate warming effect while from 90% to 99% indicate cooling effect and both effects increase from 0.25 to 0.30 μ m and increase with increase in wavelength and decrease in relative humidities and this show that adding water insoluble reflects warming on the earth atmosphere.

4.0 CONCLUSION

From the analysis of the data, it can be concluded that Angstrom exponent can be used to determine the most dominant type of aerosols. The analysis of Radiative forcing and Optical depth verify that the water-insoluble component of Continental

polluted aerosols reflects cooling effect, therefore, has a relatively high scattering coefficient. The α and α_2 shows that Earth's atmosphere is composed of dominant Fine/accumulation mode particles in the continental region, the turbidity, β , increases with

increase in RHs indicating that the aerosol loading also increases with the increase in RH and visibility of atmosphere reduces. The data clearly demonstrates that an extremely large fraction of fine/accumulation modes aerosols in turbid atmosphere mainly caused by local anthropogenic pollution or biomass aerosols transport from forest fire. The analysis showed that the inclusion of the curvature (polynomial fit

of $\ln\tau$ with respect to $\ln\lambda$) significantly improve the aerosol type discrimination whether monomodal or bimodal as found by (Eck *et al.*, 1999; Reid *et al.*, 1999; Schuster *et al.*, 2006). In our case the α_2 (curvature) is negative at all RHs, this shows that Earth's atmosphere is composed of dominant Fine/accumulation mode particles in the continental polluted aerosols.

REFERENCES

- Angstrom A.K. (1929). On the atmospheric transmission of sun radiation and on dust in the air, *Geogr. Ann.*, 11, 156–166.
- Angstrom, A. (1961). Techniques of Determining the Turbidity of the Atmosphere, *Tellus*, 13, 214–223.
- Chylek, P. and Wong, J. (1995). Effect of absorbing aerosols on global radiation budget. *Geophysical Research Letters* 22 929-931
- Eck, T. F., Holben, B. N., Reid, J. S., Dubovik, O., Smirnov, A., O'Neill, N. T., Slutsker, I and Kinne, S. (1999). Wavelength Dependence of the Optical Depth of Biomass burning, Urban and desert dust Aerosols. *Journal of Geophysical Research* 104 333-349.
- Hess M., Koepke P., & Schult. (1998). Optical properties of aerosols and Cloud: Software package OPAC., Munchen, Germany.
- Intergovernmental Panel on Climate Change (2007). Climate Change 2007: The Physical Science Basis: Contribution of Working Group I to the Fourth Assessment Report of the Intergovernmental Panel on Climate Change, edited by S. Solomon et al., Cambridge Univ. Press, Cambridge, U. K.
- King, M.D. and Byrne, D.M. (1976). A Method for Inferring Total Ozone Content from Spectral Variation of Total Optical Depth Obtained with a Solar Radiometer. *Journal of the Atmospheric Sciences*, 33, 2242-2251. [http://dx.doi.org/10.1175/15200469\(1976\)033<2242:AMFITO>2.0.CO;2](http://dx.doi.org/10.1175/15200469(1976)033<2242:AMFITO>2.0.CO;2)
- Kumar, K. R., Sivakumar, V., Reddy, R. R., Gopal, K. R., & Adesina, A. J. (2014). Identification and classification of different aerosol types over a subtropical rural site in mpumalanga, South Africa: Seasonal variations as retrieved from the AERONET sunphotometer. *Aerosol and Air Quality Research*, 14(1), 108–123. <https://doi.org/10.4209/aaqr.2013.03.0079>
- Liou, K.N. (2002). *An Introduction to Atmospheric Radiation*. Elsevier, New York, 583 p
- Mulcahy, J. P., C. D. O'Dowd, and S. G. Jennings (2009), Aerosol optical depth in clean marine and continental northeast Atlantic air, *Journal of Geophysical Research*, 114,
- Muhammad Dahiru Audu, Abdulrazak Tijjani, Ruhullahi Muhammad (2017) Analysis of Effective Hygroscopic Growths, Kelvin Effects and Water Activities of Maritime Aerosols Using Volume Mix Ratio International Research Journal of Engineering and Technology (IRJET) Volume: 04 Issue: 09 | Sep -2017
- O'Neill, N. T and Royer, A. (1993). Extraction of binomial aerosol-size distribution Radii from spectral and angular slope (Ångström) coefficients *Appl. Opt.* 32 1642-1645 17
- Pan, X. L., Yan, P., Tang, J., Ma, J. Z., Wang, Z. F., Gbaguidi, A., & Sun, Y. L. (2009). Observational study of influence of aerosol hygroscopic growth on scattering coefficient over rural area near Beijing mega-city. *Atmospheric Chemistry and Physics*, 9(19), 7519–7530. <https://doi.org/10.5194/acp-9-7519-2009>
- S. B. Muhammad, D. O. Akpootu, N. A. Yelwa, I. A. Usman, M. Abdulkadir M. A. Balarabe & A. Bala (2017). The Angstrom Exponent and Turbidity Of Water Soluble Components In The Radiative Forcing Of Urban Aerosols, *Arabian Journal of Earth Sciences*, Vol.4 - Issue 1: 18-25.
- Smirnov, A., Holben, B. N., Kaufman, Y. J., Dubovik, O., Eck, T. F., Slutsker, I., Halthore, R. N. (2002). Optical Properties of Atmospheric Aerosol in Maritime Environments. *Journal of the Atmospheric Sciences*, 59(3), 501–523. [https://doi.org/10.1175/15200469\(2002\)059<0501:OPOAAI>2.0.CO;2](https://doi.org/10.1175/15200469(2002)059<0501:OPOAAI>2.0.CO;2)
- Segan, C. and Pollack, J. (1967). Anisotropic Non-Conservative Scattering and the Clouds of Venus. *Journal of Geophysical Research*, 72, 469-477. <http://dx.doi.org/10.1029/JZ072i002p00469>
- Zhijun Wu, Jie Chen, Yu Wang, Yishu Zhu, Yuechen Liu, Bai Yao, Yuanhang Zhang and Min Hu (2018) Interactions between water vapor and atmospheric aerosols have key roles in air quality and climate change